Journal of Physics B: Atomic, Molecular and Optical Physics

PAPER

Attainable accuracies of QH^+ rotational transition frequencies (Q: ^{40}Ca, ^{24}Mg, ^{202}Hg)

IOP Publishing Journal of Physics B: Atomic, Molecular and Optical Physics
J. Phys. B: At. Mol. Opt. Phys. **53** (2020) 085401 (6pp) https://doi.org/10.1088/1361-6455/ab7425

Attainable accuracies of QH^+ rotational transition frequencies (Q: ^{40}Ca, ^{24}Mg, ^{202}Hg)

Masatoshi Kajita[1,4], Renu Bala[2] and Minori Abe[3]

[1] National Institute of Information and Communications Technology, Koganei, Tokyo 184-8795, Japan
[2] Department of Physics Indian Institute of Technology Roorkee, Roorkee-247667, India
[3] Department of Chemistry, Tokyo Metropolitan University, Hachioji, Japan

E-mail: kajita@nict.go.jp, balar180@gmail.com and minoria@tmu.ac.jp

Received 7 November 2019, revised 20 January 2020
Accepted for publication 7 February 2020
Published 18 March 2020

Abstract

Molecular rotational transition frequencies are useful as frequency standard in the terahertz region. The $X^1\Sigma(J, F) = (0, 1/2) \rightarrow (1, 1/2)$ transition frequencies of QH^+ molecular ions (Q: an even isotope of Group II element) in a linear trap are useful as measurement uncertainties are low. An uncertainty given by the Stark and Zeeman shifts can be below 10^{-15} using $^{202}HgH^+$ molecular ion.

Keywords: terahertz frequency standard, molecular ion, precise frequency measurement

(Some figures may appear in colour only in the online journal)

1. Introduction

Atomic transition frequencies in the optical and microwave regions have been measured with uncertainties of 10^{-18} [1–4] and 10^{-16} [5], respectively. The vibrational transition frequencies of homonuclear diatomic molecular ions (N_2^+, O_2^+) are also expected to be measured with uncertainties of 10^{-18} in the infrared or optical region. These frequencies are useful for the detection of variations in the proton-to-electron mass ratio [6, 7].

Establishing a frequency standard in the terahertz region (0.1—10 THz) is also useful, for example, in spectroscopic imagining including the detection of hidden paintings [8]. Solaro and collaborators measured the $^{40}Ca^+ {}^2D_{3/2}-{}^2D_{5/2}$ transition frequency (1.8 THz) with an uncertainty of 2.2×10^{-11} (dominated by the uncertainty of the Rb clock used as a reference) [9]. The vibrational transition frequencies of $^{174}Yb^6Li$ (4.17 THz) [10, 11], $^{88}Sr^6Li$ (5.06 THz), and $^{40}Ca^6Li$ (5.77 THz) [12] molecules are expected to be measured to an uncertainty of 10^{-16}. These transitions are observed using lasers to excite atomic Raman transitions in the optical region. To stabilize the frequency of a terahertz-wave source, observing a single photon electric dipole transition (E1) in the terahertz region is preferable. The stabilization of a quantum cascade laser (QCL) in the terahertz region has been performed using CH_3OH transitions to a precision of 10^{-7} [13]. This experiment was performed using CH_3OH molecules in a cell at room temperature, and therefore, the spectrum is Doppler broadened; the quadratic Doppler shift is also significant (of the order of 10^{-12}).

This paper presents estimates of the attainable accuracies of rotational transition frequencies of molecular ions in a linear trap. The linear trap uses a set of quadrupole rods to confine ions radially with an RF electric field (frequency of $\Omega/2\pi$) and a DC electrical potential on the end electrodes to confine the ions axially. Molecular ions may be sympathetically cooled via the Coulomb interaction with atomic ions, that are co-trapped and laser cooled. As the kinetic energy of ions are reduced by laser cooling, the ions localize at positions where the trap force and the Coulomb force from other ions balance. This situation produces a 'Coulomb crystal'. The ions exhibit micro-motions in the radial direction with frequency $\Omega/2\pi$ and an amplitude proportional to the radial displacement from the axis (center line of the linear rods). A small number (<50) of ions form a string crystal along the axis with a strong radial spatial confinement [14], where the trap electric field is zero. There is no micro-motion of ions in the string crystal, because there is no displacement from the axis and the trap force along the axial direction is given by a DC electric field. The amplitude of motion of the molecular ion is below terahertz wavelengths (0.3 mm), and therefore, the observed spectrum is free from Doppler broadening. The

[4] Author to whom any correspondence should be addressed.

Table 1. $X^1\Sigma v = 0(J, F) = (0, 1/2) \rightarrow (1, 1/2)$ transition frequencies f_c.

	f_c(THz)
$^{40}CaH^+$	0.282 [15]
$^{24}MgH^+$	0.382 [16]
$^{202}HgH^+$	0.390 [17]

Table 2. Description of the (J, F, M_F) states as couplings of $[M_J, M_I]$states.

(J, F, M_F)	$[M_J, M_I]$
$(0, 1/2, \pm1/2)$	$[0, \pm1/2]$
$(1, 3/2, \pm3/2)$	$[\pm1, \pm1/2]$
$(1, 3/2, \pm1/2)$	$\sqrt{\frac{2}{3}}[0, \pm1/2] + \sqrt{\frac{1}{3}}[\pm1, \mp1/2]$
$(1, 1/2, \pm1/2)$	$\sqrt{\frac{1}{3}}[0, \pm1/2] - \sqrt{\frac{2}{3}}[\pm1, \mp1/2]$

quadratic Doppler shift is less than 10^{-16} when the kinetic energy is reduced to less than 1 mK by sympathetic cooling.

Molecular ions QH^+ (Q: ^{40}Ca, ^{24}Mg, ^{202}Hg) are advantageous when measuring the rotational transition frequencies because of the simple energy structures without electron spin, electron orbital angular momentum, and Q nuclear spin (the nuclear spin of H is 1/2). The $X^1\Sigma$ $v = 0$ $(J, F) = (0, 1/2) \rightarrow (1, 1/2)$ transition (v: vibrational state, J: rotational state, and F: hyperfine state) is electric dipole (E1) allowed and the measured frequency is free of an electric quadrupole shift because $F = 1/2$ for the upper and lower states.

The outline of this paper is: section 2 estimates the attainable systematic measurement uncertainty in the $(J, F) = (0, 1/2) \rightarrow (1, 1/2)$ transition frequency, given by the Zeeman shift induced by the stray magnetic field and the Stark shift induced by the trap electric field and blackbody radiation (BBR), and section 3 describes the experimental procedure.

2. Attainable systematic uncertainty

We next present estimates of the Zeeman and Stark shifts in the frequencies for the $X^1\Sigma_{v=0}(J, F) = (0, 1/2) \rightarrow (1, 1/2)$ transition $f_c(=2B_0)$ of molecular ions $^{40}CaH^+$, $^{24}MgH^+$, and $^{202}HgH^+$ (B_v: rotational constant of the v vibrational state). The values of f_c are listed in table 1.

To estimate the Zeeman and Stark energy shifts, the states $X^1\Sigma_{v=0}(J, F, M_F)$ are obtained as couplings of states $[M_J, M_I]$, where M_P $(P = F, J, I)$ is the component of the angular momentum parallel to the magnetic field (see table 2).

The linear Zeeman shift for a magnetic field B is given by

$$\Delta f_{ZL} = (p_J M_J + p_I M_I)B, \quad (1)$$

where $p_I = 4.2$ kHz G^{-1} [18]. The value of p_J is estimated to be -1.15kHz G^{-1} [19] for the molecular ion $^{40}CaH^+$ in the $J = 1$ state, and assumed to be 15% higher for molecular ions $^{24}MgH^+$ and $^{202}HgH^+$ molecular ions (Note, p_J is proportional to the rotational angular velocity and proportional to $\sqrt{B_0}$). The linear Zeeman energy shifts in the (0,1/2, $\pm$1/2) and (1,1/2, $\pm$1/2) states of $^{40}CaH^+$ are ±2.1 kHz G^{-1} and ∓1.5 kHz G^{-1}, respectively. Therefore, the linear Zeeman shifts in the frequencies of the $(J, F, M_F) = (0, 1/2, \pm1/2) \rightarrow (1, 1/2, \pm1/2)$ and $(0, 1/2, \pm1/2) \rightarrow (1, 1/2, \mp1/2)$ transitions of $^{40}CaH^+$ are ∓3.6 kHz G^{-1} and ∓0.64 kHz G^{-1} (for $^{24}MgH^+$ and $^{202}HgH^+$ ∓4.2 kHz G^{-1} and ∓0.74 kHz G^{-1}), respectively. The linear Zeeman shift is eliminated by averaging the frequencies of the $M_F = 1/2 \rightarrow 1/2$ and $M_F = -1/2 \rightarrow -1/2$ or $M_F = 1/2 \rightarrow -1/2$ and $M_F = -1/2 \rightarrow 1/2$ transitions. Therefore, the uncertainty associated with the value of p_J is not significant in the estimation of the Zeeman shift.

The quadratic Zeeman shift Δf_{ZQ} in the $(J, F) = (0, 1/2) \rightarrow (1, 1/2)$ transition frequency, induced by the coupling between $(J, F, M_F) = (1, 1/2, \pm1/2)$ and $(1, 3/2, \pm1/2)$ states, is given by

$$\Delta f_{ZQ} = -\frac{2}{9}\frac{(-p_J + p_I)^2 B^2}{\Delta_{hf}}, \quad (2)$$

where Δ_{hf} is the transition frequency between $(1, 1/2, \pm1/2)$ and $(1, 3/2, \pm1/2)$ states. The values of Δ_{hf} for $^{40}CaH^+$ molecular ion is estimated to be 12.4 kHz [19], and the higher value by 15% is assumed also for $^{24}MgH^+$ and $^{202}HgH^+$ molecular ions (Δ_{hf} is proportional to the rotational angular velocity and proportional to $\sqrt{B_0}$). The quadratic Zeeman shift is estimated to be -513 Hz G^{-2} with $^{40}CaH^+$ molecular ion (-484 Hz G^{-2} for $^{24}MgH^+$ and $^{202}HgH^+$). With the magnetic field maintained below 1 mG, Δf_{ZQ} is less than 1 mHz. The magnetic field of several Gauss is required for laser cooling, but should be turned off at the measurement stage.

The Stark energy shift induced by the DC electric field E in the $(J, M_J') = (0, 0), (1, 0), (1, \pm1)$ states (Δf_{S-DC}) are given by $-(dE)^2/(6hB_0)$, $(dE)^2/(10hB_0)$, and $-(dE)^2/(20hB_0)$, respectively (d: permanent electric dipole moment). Here, M_P' denotes the component of P parallel to the electric field. The Stark energy shifts in the $(J, F, M_F') = (0, 1/2, \pm1/2)$ are $-(dE)^2/(6hB_0)$. The $(1, 1/2, \pm1/2)$ state is a mixture of $M_J' = 0$ and 1 with a ratio of 1:2 (table 1). The DC Stark shift in the $(1, 1/2, \pm1/2)$ state is negligible because the Stark shifts in the $M_J' = 0$ and 1 states cancel each other, although not exactly because of a centrifugal force. The (J, F, M_F) state results from a coupling of (J, F, M_F') states. Therefore, the DC Stark shift in the $(J, F) = (0, 1/2) \rightarrow (1, 1/2)$ transition frequency is $(dE)^2/(6hB_0)$. Table 3 lists the values of the permanent dipole moment d and the coefficients of fractional DC Stark shift $\Delta f_{S-DC}/(f_c E^2)$.

The electric field of the trapped molecular ions is required to be less than 0.01 V cm^{-1} to suppress the fractional DC Stark shift below 10^{-14} for the $^{40}CaH^+$ and $^{24}MgH^+$ molecular ions. The value is lower than 10^{-15} for molecular ion $^{202}HgH^+$ with an electric field of 0.03 V cm^{-1}. As shown in section 3, the electric field of the molecular ions in a string crystal has been reduced below 0.01 V cm^{-1}. The DC Stark

Table 3. Values of the permanent dipole moment d, the coefficients of fractional DC Stark shift $\Delta f_{S-DC}/(f_c E^2)$, and the magic trap rf-frequency where the Stark shift induced by the electric field of the trap cancels the quadratic Doppler shift $\Omega c/2\pi$.

	d (D)	$\Delta f_{S-DC}/(f_c E^2)$ (/(V/cm)^2)	$\Omega_c/2\pi$ (kHz)
$^{40}CaH^+$	5.31 [15]	5.78×10^{-11}	11.6
$^{24}MgH^+$	3.20 [15]	1.16×10^{-11}	42.2
$^{202}HgH^+$	0.90 [15]	8.82×10^{-13}	19.1

Table 4. Fractional Stark shift induced by BBR when the temperature of the surroundings T is 300 K. The Stark shift is induced through coupling of neighboring rotational state Δf_{BBR-R}, the neighboring vibrational state f_{BBR-V}, and the electrically excited state f_{BBR-e}.

	$\Delta f_{BBR-R}/f_c$	$\Delta f_{BBR-V}/f_c$	$\Delta f_{BBR-e}/f_c$
$^{40}CaH^+$	1.67×10^{-16}	4.96×10^{-18}	4.61×10^{-17}
$^{24}MgH^+$	1.13×10^{-16}	4.45×10^{-18}	1.86×10^{-17}
$^{202}HgH^+$	9.23×10^{-18}	1.79×10^{-18}	4.36×10^{-18}

shift is positive and cancels with the quadratic Doppler shift when electric field of the rf-trap is applied with the frequency (magic trap rf-frequency $\Omega_c/2\pi$) [20] listed in table 3.

The Stark shift induced by BBR should be considered along with shifts associated with the couplings with neighboring rotational states, vibrational excited states, and electronically excited states. The frequency shift contributed by neighboring rotational states ($J = 0$–1 and 1–2) is given by

$$\Delta f_{BBR-R} = \int \left[-\frac{2}{3}\frac{d^2(4B_0)}{(4B_0)^2 - \nu^2} + \frac{4}{3}\frac{d^2(2B_0)}{(2B_0)^2 - \nu^2} \right] \frac{\rho(\nu)}{h\varepsilon_0} d\nu,$$
$$\rho(\nu) = \frac{8\pi h\nu^3}{c^3}\frac{1}{\exp[h\nu/k_B T] - 1}. \tag{3}$$

The frequency for which $\rho(\nu)$ is a maximum is proportional to the thermodynamic temperature of the surroundings T, and is 31 THz for $T = 300$ K. At $T > 50$ K, ν is distributed mostly in the region above 3 THz, which is much larger than $4B_0$(<1 THz) and equation (3) is approximately given by

$$\Delta f_{BBR-R} = \int 32\frac{\rho(\nu) d^2 B_0^3}{h\varepsilon_0 \nu^4} d\nu$$
$$= 256 d^2 B_0^3 \frac{\pi}{\varepsilon_0 c^3} \int \frac{dx}{x[\exp(x) - 1]}. \tag{4}$$

Using equation (4), Δf_{BBR-R} is obtained to be independent to T, because of $d\nu/\nu = dx/dx$ ($x = h\nu/k_B T$). The values of $\Delta f_{BBR-R}/f_c$ are listed in table 4. The influence of the centrifugal force is one order smaller than these estimated values. The frequency shift induced by the $(\nu, J) = (0, 0) - (1, 1)$ and $(0, 1) - (1, 0)$, $(1, 2)$ couplings is given by

$$\Delta f_{BBR-V} = \int \left[-\frac{2}{3}\frac{d_{01}^2(f_\nu + 6B_1 - 2B_0)}{(f_\nu + 6B_1 - 2B_0)^2 - \nu^2} \right.$$
$$\left. - \frac{1}{3}\frac{d_{01}^2(f_\nu - 2B_0)}{(f_\nu - 2B_0)^2 - \nu^2} + \frac{d_{01}^2(f_\nu + 2B_1)}{(f_\nu + 2B_1)^2 - \nu^2} \right]$$
$$\times \frac{\rho(\nu)}{h\varepsilon_0} d\nu, \tag{5}$$

where f_ν is the vibrational transition frequency and d_{01} is the $\nu = 0$–1 vibrational transition dipole moment, both are listed in table 5. With $f_\nu \gg B_0, B_1$, equation (5) is rewritten in approximation as

$$\Delta f_{BBR-V} = \int \frac{2\rho(\nu)}{h\varepsilon_0}\frac{d_{01}^2(B_0 - B_1)}{f_\nu^2 - \nu^2} d\nu. \tag{6}$$

B_1 is 3% smaller than B_0 (table 5) [15]. The values of $\Delta f_{BBR-V}/f_c$ with $T = 300$K are listed in table 4. The frequency shift induced by couplings with state $A^1\Sigma$ is given by

$$\Delta f_{BBR-e} = \int \left[-\frac{2}{3}\frac{d_e^2(f_e + 6B_e - 2B_0)}{(f_e + 6B_e - 2B_0)^2 - \nu^2} \right.$$
$$\left. - \frac{1}{3}\frac{d_e^2(f_e - 2B_0)}{(f_e - 2B_0)^2 - \nu^2} + \frac{d_e^2(f_e + 2B_e)}{(f_e + 2B_1)^2 - \nu^2} \right] \frac{\rho(\nu)}{h\varepsilon_0} d\nu, \tag{7}$$

where f_e is the $X \rightarrow A$ transition frequency, B_e the rotational constant in the $A^1\Sigma$ state, and d_e is the $X \rightarrow A$ transition dipole moment. Values of f_e and B_e are listed in table 5. The value of d_e was estimated to be of order 2D for $^{40}CaH^+$ [21] and $^{202}HgH^+$(see section 3). The same values are assumed also for $^{24}MgH^+$. With $f_e \gg \nu$, B_0, B_e, equation (7) is rewritten in approximation as

$$\Delta f_{BBR-e} = \frac{2}{h\varepsilon_0}\frac{d_e^2(B_0 - B_e)}{f_e^2}\int \rho(\nu) d\nu. \tag{8}$$

Δf_{BBR-e} is proportional to T^4. Values of $\Delta f_{BBR-e}/f_c$ with $T = 300$ K are listed in table 4. The total fractional shift induced by BBR with $T = 300$ K is estimated to be of order 2×10^{-16}, 1.3×10^{-16}, and 1.4×10^{-17} for $^{40}CaH^+$, $^{24}MgH^+$, and $^{202}HgH^+$, respectively. As Δf_{BBR-e} is much less dominant than Δf_{BBR-R}, therefore, the uncertainty in d_e does not contribute to the total shift induced by BBR. The measurement uncertainty is dominated by the quadratic Zeeman shift and the Stark shift induced by the electric field of the trap. To reduce the measurement uncertainty below 10^{-14}, the magnetic field should be suppressed below 1 mG. Suppression is also required for the Stark shift induced by the electric field of the trap, using molecular ions in a string crystal on the axis of the linear trap (electric field <0.03 V cm^{-1}) or by trapping with magic trap frequencies (table 3). Using molecular ion $^{202}HgH^+$ is advantageous in measurements desiring low measurement uncertainties.

Table 5. The $v = 0$–1 vibrational transition frequency f_v, the $v = 0$–1 transition dipole moment d_{01}, and $(B_0 - B_1)/B_0$ (B_v is the rotational constant in the v vibrational state) are listed as well as the $X \rightarrow A$ transition frequency f_e and the rotational constant in the $A^1\Sigma$ state B_e.

	f_v(THz)	d_{01}(D)	$(B_0 - B_1)/B_0$	f_e(THz)	B_e(THz)
$^{40}CaH^+$	43.2 [15]	0.13 [15]	0.028 [15]	720 [21]	0.09 [22]
$^{24}MgH^+$	49.2 [15]	0.16 [15]	0.028 [15]	1080 [22]	0.130 [22]
$^{202}HgH^+$	58.2 [15]	0.13 [15]	0.033 [15]	1320 [22]	0.174 [22]

3. Experimental procedure

The molecular ions QH^+ are produced from the rf-trapped Q^+ ion in the chemical reaction

$$Q^+ (^1P_{1/2}) + H_2 \rightarrow QH^+ + H.$$

The excitation to the $^1P_{1/2}$ state is induced by laser light (397 nm + 866 nm for $^{40}Ca^+$, 280 nm for $^{24}Mg^+$, and 194 nm for $^{202}Hg^+$). The $^{202}Hg^+$ ion is also excited when using a $^{202}Hg^+$ discharge lamp, because only the excitation to the P state is required (not laser cooling). A $^{202}Hg^+$ discharge lamp was used in the optical pumping of $^{199}Hg^+$ ion to the $^2S_{1/2}$ $F = 0$ state (F: hyperfine state), because it is resonant with the $^{199}Hg^+$ $^2S^{1/2}$ $F = 1 \rightarrow$ $^2P_{1/2}$ $F = 0$, 1 transition (broadening is larger than the hyperfine splitting in the $^2P_{1/2}$ state) [23].

The QH^+ molecular ions are sympathetically cooled with ions, that can be laser cooled. Sympathetic cooling is effective when the mass of the molecular ion is more than 0.54 times larger that of laser cooled atomic ion [24]. The cooling effect is high when it is sympathetically cooled with Q^+ ion. For the$^{202}HgH^+$ molecular ion, sympathetic cooling with Yb^+ or Ba^+ ion seem to be easier than laser cooling of Hg^+ ion using a 194 nm laser light.

When an AC voltage $V = V_0 \cos(\Omega t)$ is applied to quadrupole rods at a distance of R from the axis, the trap force on the ion with a mass of m_i in the radial ($r-$)direction is

$$\begin{aligned} F &= m_i \omega_r^2 r \\ \omega_r &= \frac{q\Omega}{\sqrt{2}} \\ q &= \frac{4eV_0}{m_i R^2 \Omega^2} \end{aligned} \tag{9}$$

The trap is stable with $0 < q < 0.8$. The experiment is performed mainly with $\omega_r/\Omega = 0.1$–0.3. The trap force in the axial ($z-$) direction is given by

$$F_z = -m_i \omega_z^2 z. \tag{10}$$

With low kinetic energy, ions are localized to position (r_0, z_0) where the trap force and the Coulomb repulsive force balance (Coulomb crystal). Along the radial direction, there is also a micro-motion of $qr_0 \cos(\Omega t)$. When $\omega_r \gg \omega_z$, a small number of ions are localized on the axis with $r_0 = 0$ (string crystal).

The measurement is performed with a terahertz wave source, such as a QCL and a differential laser. Here, the differential laser has a difference frequency component given by a nonlinear effect of a crystal excited by two laser beams. The rotational transition may be monitored using the quantum logical method [25]. For the quantum logical measurement, the energy of mechanical motion in the axial direction of the ion should be reduced to the ground state $\hbar\omega_z/2$. Requiring $\omega_z < \omega_r < \Omega$ to form the string crystal, $\hbar\omega_z/2$ must be one order lower than $\hbar\Omega/2$. Using the quantum logical method with Ω magic trap rf-frequencies $\Omega_c/2\pi$ (table 3), is technically difficult because $\omega_z/2\pi$ should be of order of a few kiloHertz and $\hbar\omega_z/2$ is required to be of order 100 nK.

However, the Stark shift induced by the trap electric field is expected to be below 10^{-14} (10^{-15} for $^{202}HgH^+$) with any value of Ω, because the electric field of the molecular ions in the string crystal is expected to be less than 0.01 V cm^{-1} (see below). When $V_0 = 400$ V, $R = 2$ mm and $\Omega = 2\pi \times 10$ MHz with $^{40}CaH^+$ molecular ion, $q = 0.24$ and $\omega = 2\pi \times 1.7$ MHz. Then the secular motion amplitude is 0.04 μm with kinetic energy of 1 mK, and the electric field strength that the ions in the string crystal feel is 1.7×10^{-4} V cm^{-1} and the DC Stark shift is less than 10^{-17}.

For $^{202}HgH^+$, the rotational transition may be monitored with a method that is simpler than the quantum logical method. The population in the $X^1\Sigma(v, J) = (0, 1)$ state may be monitored by observing the fluorescence from laser beams of wavelengths 227 and 237 nm, because of the quasi-diagonal coupling between $X^1\Sigma$ and $A^1\Sigma$ states. To confirm the usefulness of this method, the $^{202}HgH^+$ energy structure in the $X^1\Sigma$ and $A^1\Sigma$ states was analyzed using the relativistic Kramers-restricted configuration interaction method limited to single and double excitations with the quadruple zeta quality basis sets [26]. The internuclear distance in the $X^1\Sigma$ and $A^1\Sigma$ states were found to be 0.159 nm and 0.170 nm (from [22] 0.159 nm and 1.69 nm), respectively. The transition dipole moment between $A^1\Sigma(v, J) = (0, 0) \leftrightarrow X^1\Sigma(0, 1)$, $(1, 1)$, $(2, 1)$, $(3, 1)$ states were found to be 2.1 D, 1.6 D, 0.69 D, and 0.20 D, respectively. The rate for the spontaneous emission transition is given in figure 1. Using the $A^1\Sigma(v, J) = (0, 0) \leftrightarrow X^1\Sigma(0, 1)$, $(1, 1)$ cycle transition, the probability branching fraction to dark states b_l is 0.054. Then, with measurement time τ, ratio of photon detection ϵ, and the photon scattering rate r_s, the excess noise factor F_n (ideal $F_n = 1$) is given by [27]

$$F_n = 1 + \frac{1}{r_s \tau \epsilon} + \frac{b_l}{2}\left(\frac{1}{\epsilon} - 1\right). \tag{11}$$

Taking $r_s\tau \rightarrow \infty$ and $\epsilon = 0.3$, $F_n = 1.05$, moreover, the reduction of the signal-to-noise ratio when compared with

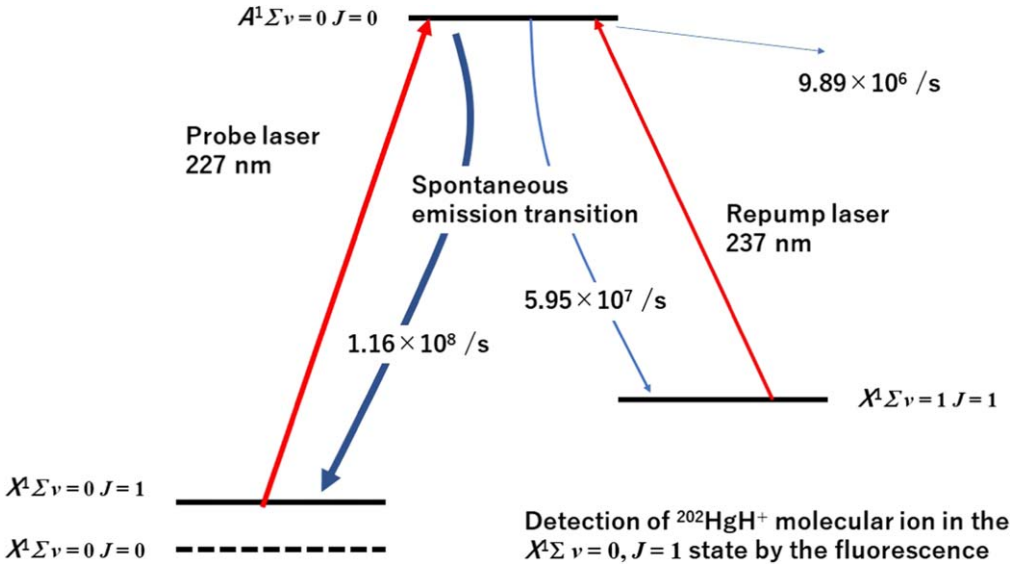

Figure 1. Monitoring the population in the $X^1\Sigma(v, J) = (0, 1)$ state by exciting to the $A^1\Sigma(0, 0)$ state using the probe and repump lasers. From the $A^1\Sigma(0, 0)$ state, the spontaneous emission transition to the $X^1\Sigma(0, 1)$, (1, 1) and other states is produced with percentages 62.5%, 32.1%, and 5.4%.

perfect cycling transition is just 5%. Fluorescence should be observed using a detector, that is sensitive to UV light only.

With this method, the mode of the mechanical motion is not required to be in the ground state, and molecular ions may be trapped with $\omega_{r,z}/2\pi = 1$–10 kHz. When molecular ions are trapped with a magic trap rf-frequency (see table 3), the Stark shift induced by the electric field of the trap and the quadratic Doppler shift cancel each other. Using molecular ions in a string crystal on the axis of a linear trap (zero electric field) is no longer required, and the measurement may be performed using molecular ions in a Coulomb crystal. Such crystals can be formed with a larger number of molecular ions (limited by the heating effect) than for a string crystal. The micro-motion in the radial direction of the molecular ions at a displaced position from the axis might induce the first Doppler effect, which is suppressed by radiation from the probe laser in the axial direction. With kinetic energy of 1 mK, the amplitude of motion of the molecular ions in the axial direction is 0.045 mm with $\omega_z/2\pi = 1$ kHz and it is much less than the wavelength of the probe laser (0.3 mm). This method is less advantageous for $^{40}CaH^+$ and $^{24}MgH^+$, because the internuclear distances for the $X^1\Sigma$ and $A^1\Sigma$ states are different by more than 15% and the $X^1\Sigma(v, J) = (0, 1)(1, 1) \longleftrightarrow A^1\Sigma(0, 0)$ transition is not cycling [21, 22]. Taking $b_l \to 1$, $F_n = 1/\epsilon$ is obtained [27].

At room temperature (300 K), only a few percent of molecular ions are in the $(v, J) = (0, 0)$ state. The $^{202}HgH^+$ molecular ion has a diagonal coupling, making it easy to pump molecular ions to the $(v, J) = (0, 0)$ state using a broadband laser beam [28]. Pumping to the $(v, J) = (0, 0)$ state using a broadband laser beam is possible also for $^{40}CaH^+$ and $^{24}MgH^+$ molecular ions, but takes longer because pumping from the vibrational excited state is also required. Using a cryogenic chamber with $T = 4$K, the population in the $(v, J) = (0, 0)$ state is 87%, 97%, and 97% for $^{40}CaH^+$, $^{24}MgH^+$, and $^{202}HgH^+$ molecular ions, respectively.

The use of a cryogenic chamber ($T < 150$ K) is required to measure the $^{202}HgH^+$ transition frequency, because the Hg vapor pressure of 0.26 Pa $T = 300$ K is too high [29].

4. Conclusion

A possible frequency standard in the terahertz region has been described that uses the $X^1\Sigma_{v=0}(J, F) = (0, 1/2) \to (1, 1/2)$ transition frequencies of the $^{40}CaH^+$, $^{24}MgH^+$, or $^{202}HgH^+$ molecular ions that are useful in the frequency stabilization of terahertz-wave sources (e.g. QCL). The measurement uncertainty is dominated by the Stark shift induced by the electric field of the trap and the quadratic Zeeman shift. Using molecular ions in a string crystal along the axis of a linear trap is required, and hence the electric field of the trap must be below 0.03 V cm^{-1}. A magnetic field below 1 mG is also required to be maintained.

The $^{202}HgH^+$ transition frequency seems to be the most advantageous for measurements because uncertainties remain below 10^{-15}. This transition is also advantageous in monitoring fluorescence from the many molecular ions trapped by the rf-electric field at this frequency because the Stark shift induced by the electric field of the trap cancels the quadratic Doppler shift.

Acknowledgments

This research was supported by a Grant-in-Aid for Scientific Research (B) (Grant No. JP 17H02881), and Grants-in-Aid for Scientific Research (C) (Grant No. JP 17K06483) from the Japan Society for the Promotion of Science (JSPS). RB thanks Dr H S Nataraj of IIT Roorkee, India for helpful discussions. Theoretical calculations reported in this work were performed on the computing facility in the Department of Physics, IIT Roorkee, India. This work was also supported

by Department of Science and Technology, Inspire and FIST division, India (Grant No. SR/FST/PS1-148/2009(C)). We thank Richard Haase, PhD, from Edanz Group (edanzediting.com/ac) for editing a draft of this manuscript.

ORCID iDs

Masatoshi Kajita https://orcid.org/0000-0002-2143-396X

References

[1] Ushijima I, Takamoto M, Das M, Ohkubo T and Katori H 2015 *Nat. Photon.* **9** 185
[2] Nicholson T *et al* 2015 *Nat. Commun.* **6** 6896
[3] Chou C W, Hume D B, Koelemeij J C J, Wineland D J and Rosenband T 2010 *Phys. Rev. Lett.* **104** 070802
[4] Huntemann N, Sanner C, Lipphardt B, Tamm C and Peik E 2016 *Phys. Rev. Lett.* **116** 063001
[5] Weyers S, Gerginov V, Kozda M, Rahm J, Lipphardt B, Dobrev G and Gibble K 2018 *Metrologia* **55** 789
[6] Kajita M, Gopakumar G, Abe M, Hada M and Keller M 2014 *Phys. Rev.* A **89** 032509
[7] Kajita M 2017 *Phys. Rev.* A **95** 023418
[8] Fukunaga K, Ogawa Y, Hayashi S and Hosako I 2007 *IEICE Electron. Express* **4** 258
[9] Solaro C, Meyer S, Fisher K, DePalatis M V and Drewsen M 2018 *Phys. Rev. Lett.* **120** 253601
[10] Kajita M, Gopakumar G, Abe M and Hada M 2011 *Phys. Rev.* A **84** 022507
[11] Kajita M, Gopakumar G, Abe M and Hada M 2012 *Phys. Rev.* A **85** 062519
[12] Kajita M, Gopakumar G, Abe M and Hada M 2013 *J. Phys. B: At. Mol. Opt. Phys.* **46** 025001
[13] Ren Y, Hayton D J, Hovenier J N, Cui M, Gao J R, Klapwijk T M, Shi S C, Kao T-Y, Hu Q and Reno J L 2012 *Appl. Phys. Lett.* **101** 101111
[14] Alighanbari S, Hansen M G, Korobov V I and Schiller S 2018 *Nat. Phys.* **14** 555
[15] Abe M, Kajita M, Moriwaki Y and Hada M 2010 *J. Phys. B: At. Mol. Opt. Phys.* **43** 245102
[16] Leininger T and Jeung G H 1995 *J. Chem. Phys.* **103** 3942
[17] Huber K P and Herzberg G 1979 *Constants of Diatomic Molecules* (New York: Van Nostland)
[18] Vanier J and Audoin C 1989 *The Quantum Physics of Atomic Frequency Standards* (Bristol: Hilger) p 24
[19] Chou C W, Kurz C, Hume D B, Plessow P N, Leiblandt D R and Leibfried D 2017 *Nature* **545** 203
[20] Madej A A, Dube P, Zhou Z, Bernard J E and Gertsvolf M 2012 *Phys. Rev. Lett.* **109** 203002
[21] Abe M, Moriwaki Y, Hada M and Kajita M 2012 *Chem. Phys. Lett.* **521** 31-35
[22] NIST Standard Reference Database Number 69 (https://webbook.nist.gov/chemistry/)
[23] Major F G and Werth G 1973 *Phys. Rev. Lett.* **30** 1156
[24] Baba T and Waki I 2002 *Appl. Phys.* B **74** 375
[25] Schulte M, Loerch N, Leroux I D, Schmidt P O and Hammerer K 2016 *Phys. Rev. Lett.* **116** 013002
[26] Bast R *et al* 2015 DIRAC, a relativistic ab initio electronic structure program, Release DIRAC15
[27] Lasner Z and DeMille D 2018 *Phys. Rev.* A **98** 053823
[28] Stollenwerk P R, Kokish M G, de Oliveira-Filho A G S, Ornellas F R and Odom B C 2018 *Atoms* **6** 53
[29] Hicks W T 1963 *J. Chem. Phys.* **38** 1873